Magnetic thin films in recording technology

by V. S. Speriosu D. A. Herman, Jr. I. L. Sanders T. Yogi

This paper is a review of recent progress in magnetic thin films for use in recording media and heads. Emphasis is on work that has been carried out at IBM. Topics covered include thin-film media for high-density recording, laminated soft-magnetic films for controlling domains and extending the frequency range of inductive heads, exchange-biasing of magnetoresistive sensors, and magnetic multilayer structures.

Introduction

The progress of magnetic disk data storage toward higher areal densities has been facilitated by the development of thin-film recording heads—introduced by IBM in the late 1970s—and thin-film recording media. The latter are currently displacing particulate coatings in many applications, and are expected to provide the basis for reaching storage densities in excess of one gigabit per square inch by the end of the 1990s. In order to achieve these densities, continued advances will be required in

**Copyright 1990 by International Business Machines Corporation. Copying in printed form for private use is permitted without payment of royalty provided that (1) each reproduction is done without alteration and (2) the Journal reference and IBM copyright notice are included on the first page. The title and abstract, but no other portions, of this paper may be copied or distributed royalty free without further permission by computer-based and other information-service systems. Permission to republish any other portion of this paper must be obtained from the Editor.

magnetic film storage device performance (in both heads and media) and in our understanding of the fundamental physical processes governing device behavior. This review includes discussions of some of the challenges to be faced in achieving these goals.

· Scaling trends

The reduction during the past twenty years in the linear dimensions of the bit cell in magnetic disk storage systems is shown in Figure 1. The data are derived from various IBM "high-end" products from the 2314 disk file (introduced in 1966) to the recent 3390 disk file, but the trends are generally representative of the substantial decrease in unit bit-cell dimensions which has occurred in magnetic data storage devices during this period. The area of a unit cell is given by the product of the bit length (determined by the linear recording density and influenced by such parameters as head gap, head-media separation, and magnetic characteristics of the recording medium) and the track pitch (determined by the distance between track centers, which in turn is dictated by the width of the recording element and the guardband between adjacent tracks). We anticipate that cell dimensions will continue to decrease over the next decade, as shown in the figure. This trend is already in evidence today, driven by the introduction of thin-film metal media with their high linear density potential, and thin-film heads which should permit very narrow track widths to be achieved. Thus, we can reasonably expect linear recording densities of 4000 fc/mm

186

(flux-changes per millimeter) or $1/4~\mu m$ bit length and a track pitch in the 2- μm range to be realized by the end of the decade. Such intensive scaling trends impose stringent requirements on both head and media materials.

• Limits to recording performance

In this review, we concentrate on magnetic films of interest in longitudinal magnetic recording, in which the magnetization is largely confined to the plane of the medium. This is in contrast to the perpendicular magnetic recording mode, in which the magnetization lies normal to the plane of the medium [1]. The preferred recording medium for perpendicular magnetic recording has typically been a cobalt-chromium sputtered film with a normal anisotropy sufficient to overcome the demagnetizing field $(H_k > 4\pi M_s)$, where H_k is the anisotropy field and M_s is the saturation magnetization). The most promising results have been achieved using a single-pole head [2], to emphasize the field component normal to the film plane. In this approach a relatively thick soft-magnetic layer is deposited beneath the recording medium, and effectively forms part of the flux path of the head. The relative merits and density potential of longitudinal and perpendicular magnetic recording are still the subject of much debate, although modeling suggests that the performance differences at short wavelengths (that is, at a high linear density) may not be large [3]. The reader is referred to [4] for a comprehensive review of perpendicular magnetic

The width of a written transition is the lower bound on cell bit length. Various models have been proposed to predict the width of a written transition in a longitudinal recording medium [5, 6], although none deal adequately with the micromagnetic characteristics of thin metallic films. A review of the physical origins of the limits in polycrystalline thin-film media has been published recently [7]. Signal output is determined by the product of remanent magnetization and film thickness (M,t), where Mis the remanent magnetization and t is the film thickness), and it is generally accepted that the transition width in film media scales in some fashion with $M_{e}t/H_{o}$ [8] (H_{o} being the coercivity), so that a very thin film with a high coercivity and remanent moment is required for high-density longitudinal recording with high output. However, the microstructural features of the film must be taken into account in any detailed study. Specifically, it is the switching behavior of clusters of grains in the films which complicates the analysis. This influences the regularity of the domain boundary between the recorded bits, and the effect is to produce random shifts (peak jitter) in the location of the output signal for each transition. The peak jitter in the reproduced signal is a major factor limiting the performance in high-density recording media. It is shown below that the intrinsic media noise originating in the

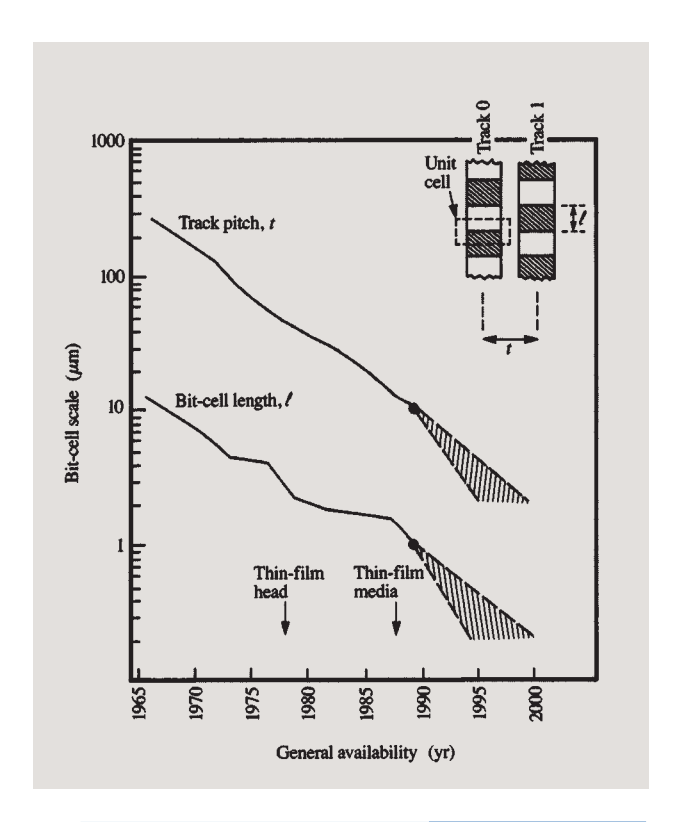
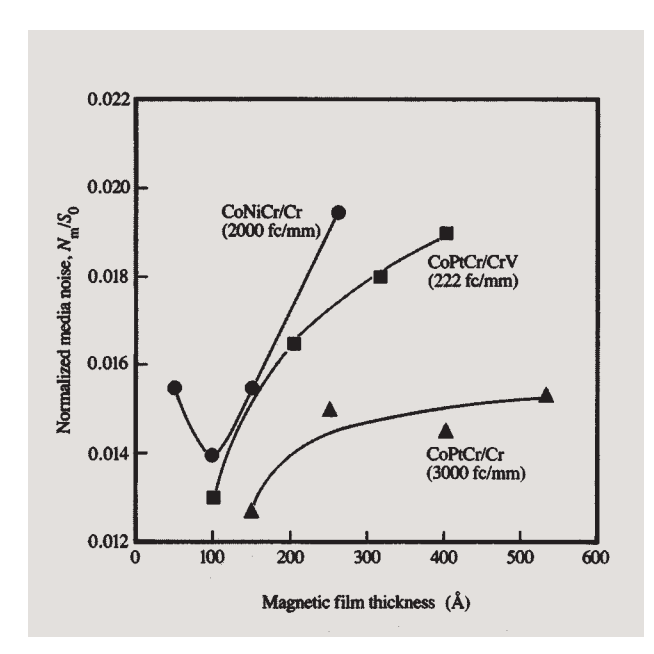


Figure 1
Scaling trends for magnetic disk storage systems.

transitions can be reduced by generating film structures exhibiting an isolated granular structure with reduced exchange coupling across grains. While analytical continuum models predict a broadening of the transition with a lower hysteresis squareness due to the decoupling of the grains, the suppression of grain clusters will almost certainly influence the sharpness of the written transitions. In addition, the lower squareness has an impact on the overwrite performance (the degree to which the residual signal associated with old information is reduced when overwritten by new data), and a balance in film properties must be achieved for optimum overall recording performance. For these reasons, the physical limit to the size of the minimum bit-cell length (and hence maximum linear recording density) that can be supported in a metalfilm medium cannot yet be precisely predicted and must therefore be determined experimentally. From a practical point of view, experiments of this kind are often unsatisfactory because of the constraints imposed by the geometry of the recording head and the finite spacing between it and the medium; further work in this area is necessary.

Factors limiting the width of the recorded bit cell are more difficult to quantify because they are primarily



Variation of normalized media noise with film thickness. The integrated media noise $N_{\rm m}$ is normalized to the isolated signal (pulse) amplitude S_0 and is shown as a function of Co-alloy media film thickness. From [22], reproduced with permission. © 1989 IEEE.

system-dependent. The ratio of the signal to the media noise scales with the square root of the track width [9] (in other words, this ratio degrades by 3 dB for a halving of the track width). At some point, determined by system noise considerations, insufficient signal is available for error-free data recovery. Another factor is the residual noise present at the edges of a recorded track [10], which becomes increasingly important as track width is reduced. However, recent work in which the tracks are physically defined in the film media, eliminating edge noise, suggests that reasonable signal-to-noise performance can be achieved even at a submicron track width [11]. Track density limitations are perhaps more strongly influenced by the film head technology, where the problem is one of maintaining head efficiency and frequency response with decreasing track width. The domain configuration in the pole tips of an inductive thin-film head is a critical factor in determining head stability and performance, particularly at narrow track width, and lamination of the soft-magnetic film (usually Permalloy) is a possible method of eliminating domain walls in the films [12]. Nevertheless, it has recently been shown that satisfactory domain control can be achieved in a single-layer film down to a 2-\mu m track width [13]; continued progress in materials selection and processing is anticipated.

Exploratory media

• High-density media

In order to achieve areal densities of 0.5-1.0 Gb/in², roughly an order of magnitude greater than at present, the media must be able to support linear densities of ~4000 fc/mm with adequate signal-to-noise and overwrite ratios. As the space between the recording transitions decreases, we expect the microstructural details of the media to become increasingly important because of their polycrystalline nature. The complexity of thin-film media on a microscopic scale has prompted extensive investigations of the relationship between their microstructure (grain morphology, grain size, and crystallographic orientation), magnetic properties (coercivity H_c , saturation magnetization M_s , remanent magnetization M_r , coercive squareness S^*) and recording performance (noise, overwrite, and linear resolution). In this section, we review recent advances in the understanding of media properties based on microstructural characterization, micromagnetic imaging, and theoretical micromagnetic model calculation, with emphasis on the media noise characteristics of Co-based allovs.

In addition to the alloying of cobalt with other elements to satisfy functional requirements, underlayers have been used effectively to "tailor" the magnetic and recording characteristics of Co-alloy media [14-16]. The relationship between microstructure and media noise was investigated for CoNiCr alloys on Cr underlayers [16]. The media noise showed a substantial decrease, a factor of ten in noise power, as the Cr thickness increased from 10 to 100 nm. This effect was explained by the development of columnar morphology in the Cr film which was replicated into the CoNiCr layer, resulting in a partial physical separation of CoNiCr grains and hence a reduction in intergranular exchange coupling. This interpretation is consistent with the results of micromagnetic calculations [17, 18] in which reduced intergranular exchange coupling leads to transitions with zigzag domains of smaller amplitude and to smaller uncertainty with respect to the position of written transitions. The experimentally observed enhancement in H_c and reduction in S^* were also consistent with the predictions of this model. Similar trends in media noise and magnetic properties have been observed in other materials systems such as CoP/Cr [19], CoCr ternary alloys/Cr [20], and CoPtCr alloys/Cr [21].

Reduction of the intrinsic transition parameter (a function of $M_r t/H_c$) permits the media to support higher linear density; thus, scaling trends are toward the use of thinner films, with the constraint that sufficient signal (proportional to $M_r t$) must be available for error-free detection. Magnetic and recording characteristics of very thin metal-film media were recently reported [22]. CoPtCr

and CoNiCr alloys on Cr or CrV underlayers were studied in the magnetic layer thickness range of 5-50 nm. A systematic reduction in the normalized media noise was observed at all densities up to 3000 fc/mm as the magnetic film thickness decreased (Figure 2). As can be seen, the integrated media noise voltage $N_{\rm m}$ normalized to the isolated pulse amplitude $S_{\rm 0}$ decreases with decreasing media film thickness. On the basis of microstructural analysis, it was suggested that the isolation of magnetic grains during the nucleation stage and their subsequent coalescence were responsible for the observed dependence. It was also noted that the S^* decreased with the reduced magnetic film thickness, which is consistent with a reduced exchange coupling based on micromagnetic modeling.

The importance of exchange coupling in the transition noise of longitudinal media has been demonstrated with micromagnetic modeling [17, 18] and experimentally substantiated with morphological studies of magnetic grains and their recording noise performance [7, 16]. Since the reduction of ferromagnetic exchange coupling in the magnetic media results in the lowering of the coercive squareness, one would expect a correlation between the media noise and S* for the instances in which the exchange coupling is the dominant noise mechanism. A correlation was found [23] between the media noise and S* for a wide variety of Co-alloy longitudinal media as well as for sputtered y-Fe,O, media, as shown in Figure 3. Similar correlations have been reported for CoPtNi [7] and CoP [24]. It should be emphasized, though previously mentioned [23], that the lowering of S^* does not always lead to the reduction of media noise. Other mechanisms, such as preferred out-of-plane orientation of the c-axis of Co-alloy grains, can induce the lowering of S^* without the simultaneous reduction of media noise. For example, a cobalt-alloy film deposited on a W underlayer can cause such lowering [15].

The above discussion of media noise does not address other important aspects of recording performance such as overwrite and signal amplitude. A previous study of sputtered γ -Fe₂O₃ media points out the importance of the role of S^* in other recording parameters such as peak shift and linear resolution [25]. Thus, to attain high-density recording with Co alloys, the media must similarly be optimized for various and often conflicting recording requirements.

• Analysis techniques for media studies Conventional structural analysis techniques such as X-ray diffraction (XRD) and transmission electron microscopy (TEM) provide useful information on crystallographic orientation, grain morphology, and other microstructural characteristics of thin-film media. On the other hand, written transitions in film media are primarily determined

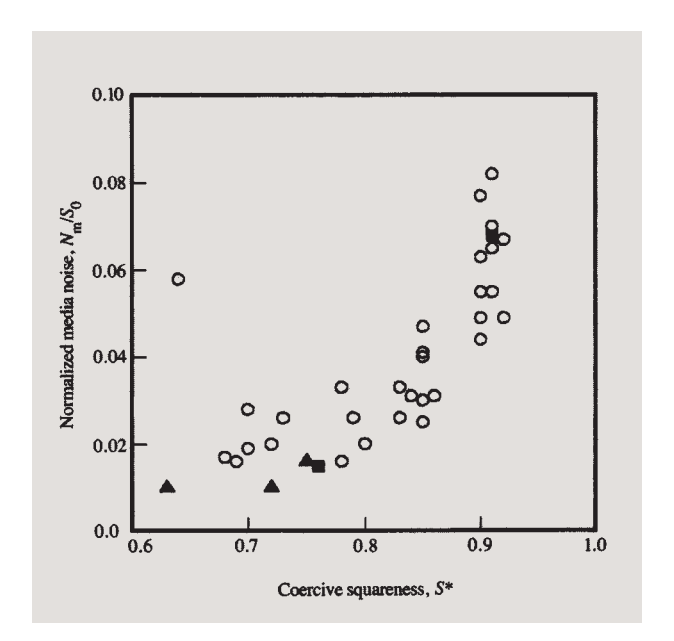
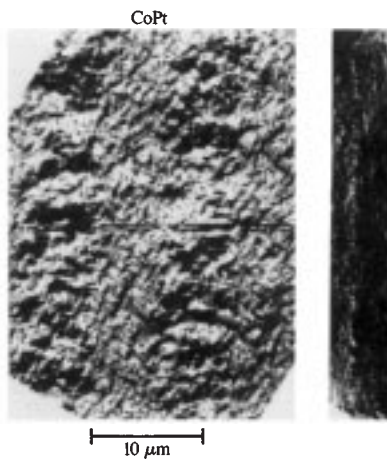


Figure 3

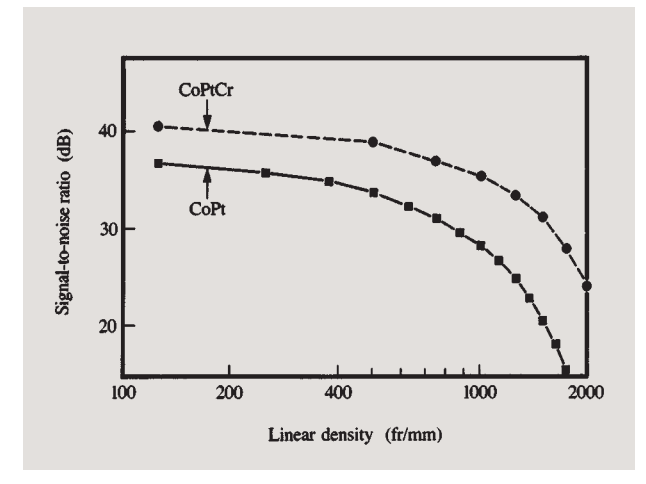
Normalized media noise versus coercive squareness at 3000 fc/mm. From [23], reproduced with permission.

by local magnetic interactions of the magnetic grains in the film. Several techniques have been used to image microscopic magnetic configurations in thin-film media. They include Lorentz microscopy [25, 26], magnetic force microscopy [27, 28], scanning electron microscopy with polarization analysis [29], and electron holography [30]. Representative examples of some of the above techniques are reviewed for the cases in which micromagnetic transition images have been related to recording characteristics of thin-film media.

Lorentz electron microscopy has been used to image the micromagnetic structure of remanent and recorded transition regions. In general, thin-film recording media exhibit highly complex micromagnetic patterns. In the recorded transition regions, the domain boundaries can vary from a zigzag configuration, as observed in an obliquely evaporated FeCoCr alloy film [31], to the more complex combination of vortices and featherlike domain structures in a sputtered Co-alloy film [26]. Figure 4 illustrates the use of Lorentz electron microscopy in the Foucault mode to image the micromagnetic configuration of recorded bit cells in CoPt and CoPtCr alloy films. It is apparent that the written transitions show better spatial definition in the CoPtCr alloy than in the CoPt alloy; this is reflected in superior signal-to-noise performance at all transition densities, as shown in the bottom graph of the figure.







Illustrative use of Lorentz electron microscope in Foucault mode to image the micromagnetic configuration of recorded bit cells in CoPt and CoPtCr films. The direction of recorded magnetization is indicated by the arrows in the micrographs; the track edges are seen at the top and bottom of the micrographs. By the courtesy of P. S. Alexopoulos et al.

Magnetic force microscopy, a relatively new imaging technique, alllows the imaging of recorded transitions with minimal sample preparation. The technique has been used to study magnetic recording behavior of Co-alloy thin-film media with sub-100-nm resolution [32, 33]. The technique is illustrated in Figure 5, which shows recorded bit patterns in Co-Sm media for which the signal-to-noise ratio degraded with increasing density more rapidly than observed in other Co-alloy media. Other images obtained using the technique show progressive loss in the transition definition with the increase in linear density and give qualitative confirmation of the recording results. As the areal density in magnetic recording increases, we expect

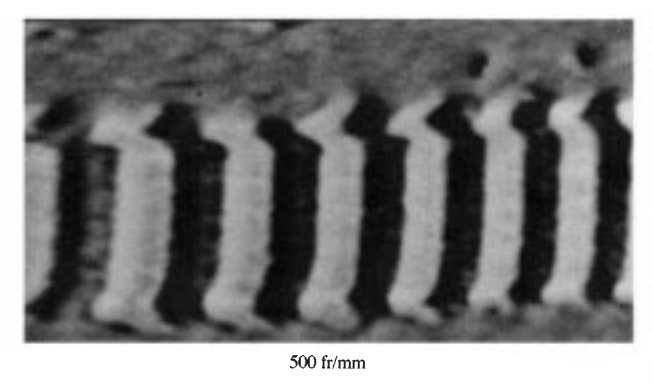
that imaging techniques will play an increasingly important role in developing an understanding of the detailed relationship between the microstructure and recording performance of thin-film media.

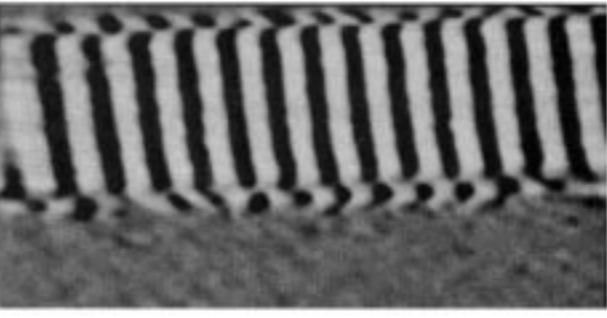
Finally, as reported recently [34-36], some of the understanding of the relationships among the media microstructure, magnetic properties, and recording performance which has been acquired has been applied to the development and optimization of thin-film media that can support recording areal densities as high as 1.2 Gb/in². The thin-film disk structure, carbon/CoPtCr/Cr, was utilized in combination with dual-element heads (inductive write and magnetoresistive read) and a partial-responsemaximum-likelihood channel in order to sustain the high areal density. The magnetic properties of the media were optimized by adjusting the film thickness, alloy composition, and deposition conditions to achieve high linear density resolutions (up to 5000 fc/mm), low transition jitter (down to 5 nm for 3-\mu m track widths), and high overwrite ratios (above 40 dB). The media noise reduction, in particular, was attained by controlling the film growth morphology such that the intergranular exchange coupling was minimized by the isolation of the magnetic grains.

• Laminated-film media for noise reduction

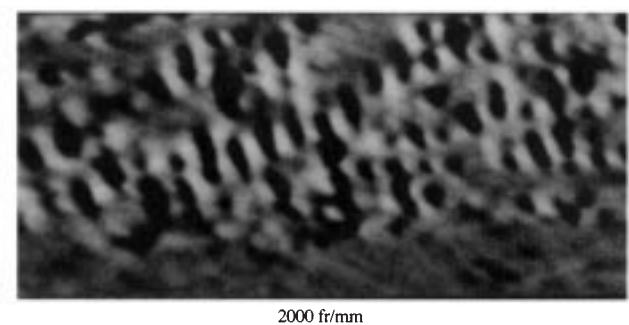
The use of laminated film structures has been proposed as a method of increasing coercivity for a given magnetic layer thickness [37] presumably because of favorable morphology in the individual, thinner magnetic layers. As indicated above, it was recently demonstrated that thinner films ($\approx 100 \text{ Å}$) exhibit a lower normalized media noise than do thicker magnetic layers. An interesting extension of this phenomenon is to combine several very thin layers into a low-noise medium with an $M_r t$ of interest for recording applications [38]. Combining several of these thin layers permits signal amplitude to be maintained (signal is proportional to $M_r t$) while retaining the low-noise characteristics of the thin layers. In addition, if the noise in the layers is uncorrelated, a further reduction in overall media noise is achieved by decoupling the layers.

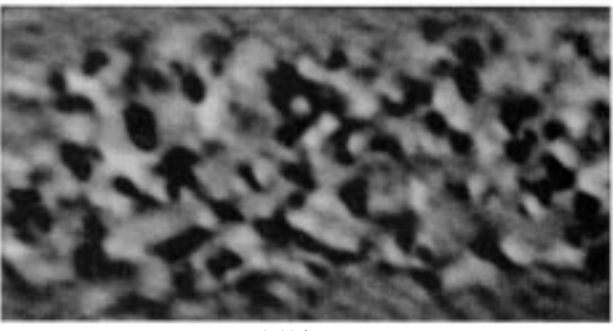
Results comparing the performance of a conventional structure employing a single layer of CoPtCr (550 Å thick) and a CrV underlayer with multilayer films comprising 2, 4, and 6 layers interrupted by spacers of CrV, each 30 Å thick, are shown in Figure 6. The coercivity and product of the remanent magnetization and thickness are similar (\sim 1200 Oe and \sim 2.0 \times 10⁻³ emu/cm², respectively), but a substantial improvement in signal-to-noise ratio for the laminated films is observed. The greatest effect is seen when the single layer is replaced by two layers, but incremental improvements are evident even for the six-layer structure. It is also observed that the coercive squareness decreases monotonically as the number of





1000 fr/mm





3000 fr/mm

Figure 5

Illustrative use of magnetic force microscopy to image the magnetization patterns of recorded bit cells in Co-Sm alloy media at various densities. Note the poor definition of the recorded transitions at high densities, which corresponds to poor SNR performance. By the courtesy of H. J. Mamin et al.

layers increases, consistent with arguments for decoupled structures outlined above. Other aspects of the recording performance, such as the isolated pulse characteristics, resolution, and overwrite are comparable to those of single-layer films, indicating that the laminated structures behave much like single-layer films having comparable $M_{\rm r}t$ values.

• Patterned film media

The possibility of etching the surface of a magnetic disk to physically define the location of each data track was proposed in 1963 [39]. The principal motivation of the proposal was to increase the tolerance of the recording system to head-repositioning errors in a fashion which did not require use of a separate write head that was wider than the read head. With the present trend toward thin-film recording materials (and the concurrent trend toward smaller disk diameters), the use of photolithographic techniques for media patterning has become more attractive. Recently, studies have concentrated on the scaling of magnetic recording characteristics to sub- μ m track widths for both Co-alloy and sputtered γ -Fe₂O₃ films using photolithographic patterning [9]. At such narrow track widths, there are several potential advantages in

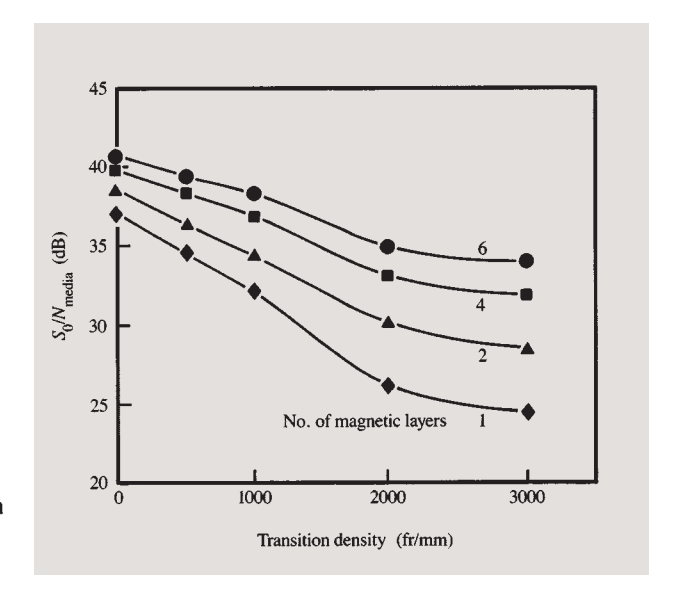
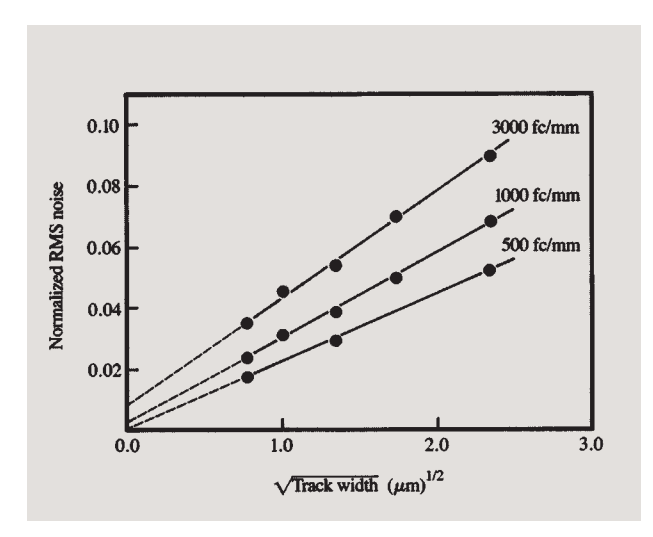


Figure 6

Ratio of isolated pulse signal to media noise versus transition density for films containing 1, 2, 4, and 6 layers. From [38], reproduced with permission. © 1990 IEEE.



Normalized RMS noise versus the square root of the track width for several recording densities. From [9], reproduced with permission. © 1987 IEEE.

patterning the recording media: enhanced head-positioning capability, suppression of noise due to the absence of unerased data in the guardband between adjacent tracks, and reduction of the magnetically induced noise present along the edges of recorded tracks. The major question facing the system designer is to determine the areal density at which advantages outweigh the complexity and cost of the patterning process.

Fabrication of discrete tracks in thin-film media has been described elsewhere [9]. The parameter of interest from a recording viewpoint, as the bit cell is reduced in size, is the scaling of the signal-to-noise ratio in the readback signal. Investigation of magnetic recording performance at very narrow track width has been limited in previous studies by the availability of suitable recording heads. The discrete track approach allows relatively wide heads to be used for writing and reading, provided that the tracks are spaced sufficiently far apart to avoid interference. It is found that the signal amplitude scales linearly with track width, confirming that conventional scaling is applicable for signals from patterned tracks having widths at least as narrow as $0.5~\mu m$.

Simple scaling theory for media noise [38], assuming that the noise is uncorrelated across the width of the track, predicts that the noise power should be proportional to the volume of media contributing to the noise; in other words, that the noise *voltage* should scale linearly with the square root of the track width. A typical plot of media noise as a function of track width is given in Figure 7, at various recording densities. The data have been normalized to the

amplitude of an isolated readback pulse from the same head on an unpatterned portion of the disk. A linear variation with the square root of track width is indeed found at all recording densities, confirming that there are no apparent correlations of the noise for track widths larger than 0.5 μ m. The applicability of such a straightforward scaling law suggests that the magnetic domain structure is uniform across the track, with no gross irregularities at the edges. The implication is straightforward: Given that the signal is proportional to the track width and the noise is proportional to the square root of the track width, the signal-to-media noise also scales as the square root of the track width, to track widths as narrow as 0.5 μ m. This gives reason for optimism that systems using thin-film media with track widths in the 1- μ m range will be achievable in the future.

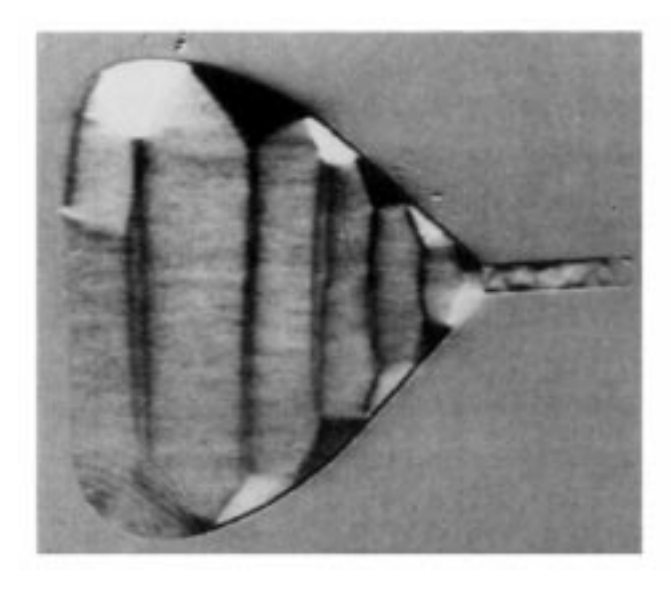
Amorphous films

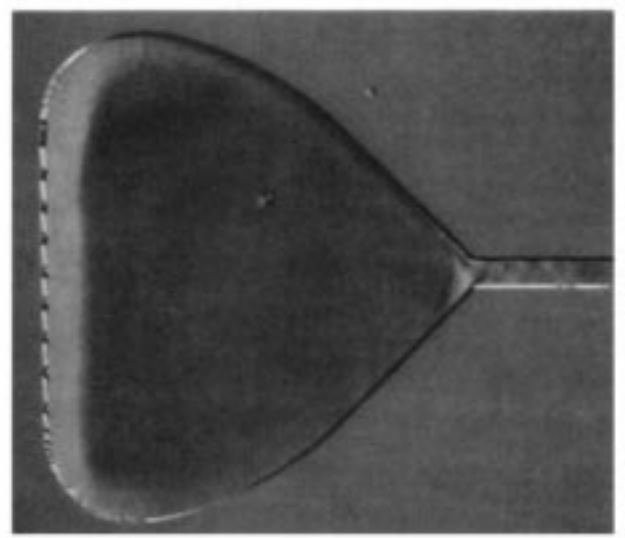
It is known that amorphous films can be prepared with macromagnetic properties in the range of interest for high-density longitudinal recording. In that regard, films of CoSm [40] and TbFeCo [41] have received the most attention to date. Little detailed information has been published on the noise performance of such noncrystalline films, although it has been shown that films of CoSm, for example, exhibit anomalous behavior [42]; however, it is uncertain whether this is a result of the anisotropic nature of the films (these media often have pronounced anisotropies introduced by the deposition configuration or by substrate effects) or of the amorphous structure of the films. Nevertheless, the amorphous rare-earth alloys warrant further study for possible applications in this area and are the subject of continued study [43].

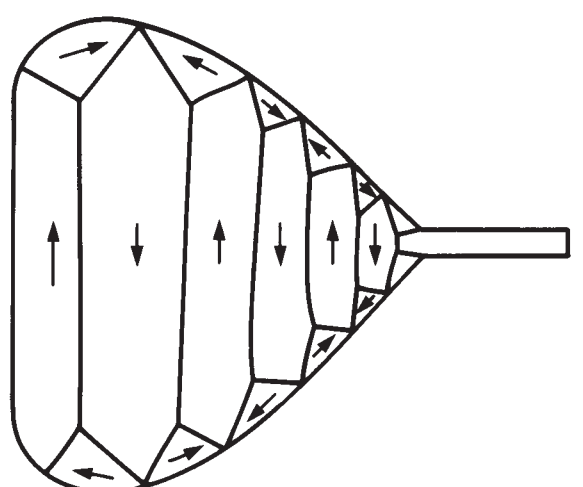
Laminated soft-magnetic materials for heads

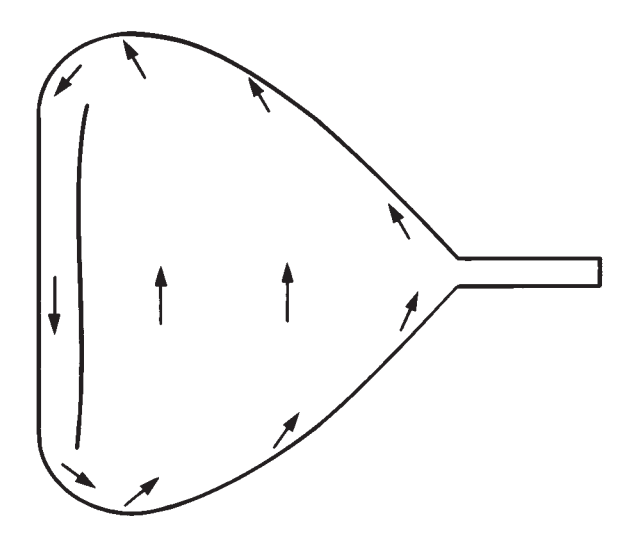
Currently thin-film inductive and magnetoresistive (MR) heads are produced almost exclusively with plated or sputtered Permalloy (NiFe) yokes having thicknesses of about 1–2 μ m. To achieve projected densities and channel rates, yoke materials need to be improved in three aspects: Increased domain stability is needed for narrow pole tips, increased saturation magnetization is needed to record on higher-coercivity disks, and permeability roll-off frequency must be increased. Replacing single-layer yokes with laminations having nonmagnetic insulators, so as to yield magnetostatically (not exchange) coupled layered structures, offers improvements with regard to the first and third areas. New high-moment, laminated materials are being developed to address all three areas.

Lamination has long been recognized as helpful for improving the high-frequency performance of bulk soft-magnetic materials by reducing eddy-current damping. For small devices such as thin-film recording heads, micromagnetic effects must also be considered. Closure









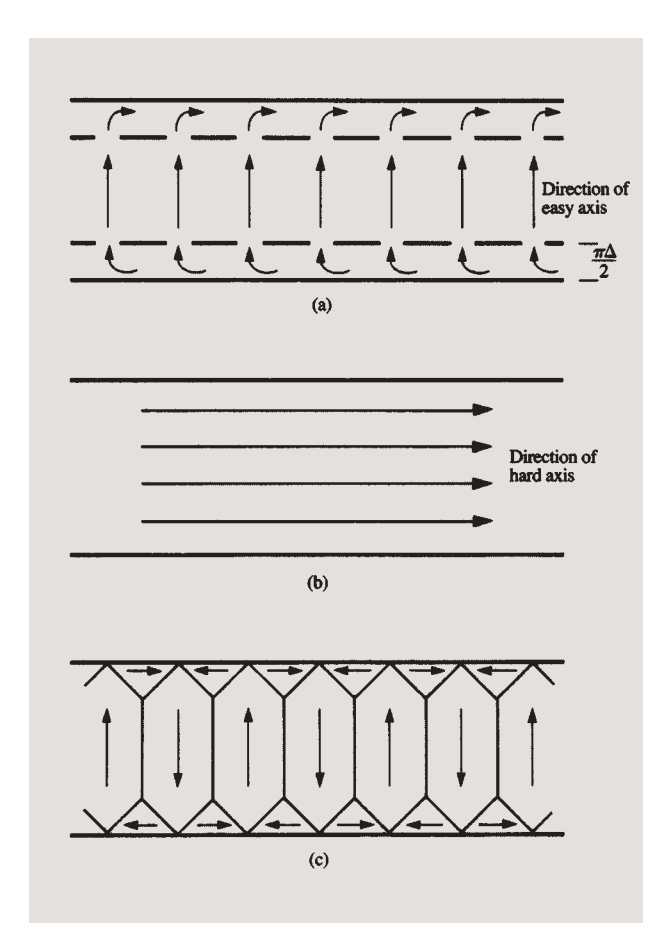
Domain wall patterns for single-layer (left) and laminated (right) thin-film-head-yoke shaped elements (pole tip region is not laminated). The upper images were taken with a LAser Magneto-Optic Microscope (LAMOM). The lower sketches contain inferred magnetization directions and domain walls. From [12], reproduced with permission. © 1988 IEEE.

domains can lead to wall-motion-induced noise, reduced response at high frequencies, and domain configuration instabilities [12, 44-46]. Some years ago concerns regarding these effects led to experiments with laminated soft-magnetic films, in which flux closure was expected between pairs of the magnetic sheets. Early results were promising; e.g., laminated strips had no closure domains (180° walls were present) and had no permeability roll-off at high frequencies [46]. In a thin-film head with laminated tips, produced in 1970 [45], the pole pieces appeared to have no domain walls, and a two-port structure consisting

of two heads with pole pieces in contact had a 60-MHz bandwidth. As seen in Figure 8, recent results [12, 47, 48] have confirmed that most domain walls can be eliminated in a typical recording head yoke by lamination. Several groups have reported fabrication of heads with laminated yokes [49, 50]; in particular, the head described in [49] performed well, with very low noise in readback.

• Understanding

Building on a background in coupled magnetic layers [51], Slonczewski et al. [12] have developed a model for



Micromagnetic states predicted by the Slonczewski et al. model: (a) easy-axis state; (b) hard-axis state; (c) Bloch-wall state. From [12], reproduced with permission. © 1988 IEEE.

laminated, magnetostatically coupled (not exchange-coupled) long stripes with relatively thick layers (such that a single layer can support Bloch walls). Depending on geometric and materials parameters, the model predicts the existence of the "easy-axis" state of Figure 9(a), the "hard-axis" state of Figure 9(b), or the "Bloch-wall" state of Figure 9(c).

• Edge-curling walls (ECWs)

A key contribution of the model cited above is the prediction of the behavior of the magnetization M near an edge that is not parallel to the magnetic easy axis. There the model predicts that M should curl both in a direction normal to the plane of the films for closure in adjacent magnetic layer(s) and in in-plane directions (to avoid edge poles), leading to the "edge-curling" description [see Figure 10(a)]. To derive equations describing this M

curling, the approximate stray-field-free magnetostatic energy was minimized for θ [\equiv arctan (M_x/M_y) , the x-y projection of M in the lower film with respect to the film edge, x=0]; $\theta=\theta_{\rm E}$ defines the easy-axis direction of magnetic anisotropy. Figure 10(b) describes the manner in which the x-y projection of M is expected to curl near the film edge, while distributing flux closure over the spacer. In the case in which the anisotropy field is normal to the edge ($\theta_{\rm E}=90^{\circ}$), the model predicts a discrete edge-curling wall/region with a width $(\pi\Delta/2)$, where $\Delta=M_{\rm S}(\pi bD/K)^{1/2}$; D and b are the magnetic layer and spacer thicknesses shown in Figure 10(a); $M_{\rm S}$ is the spontaneous magnetization, and K is the uniaxial anisotropy constant. Figure 11 shows predicted variations of $(\pi\Delta/2)$ for Permalloy. For anisotropy other than normal to the edge, the model

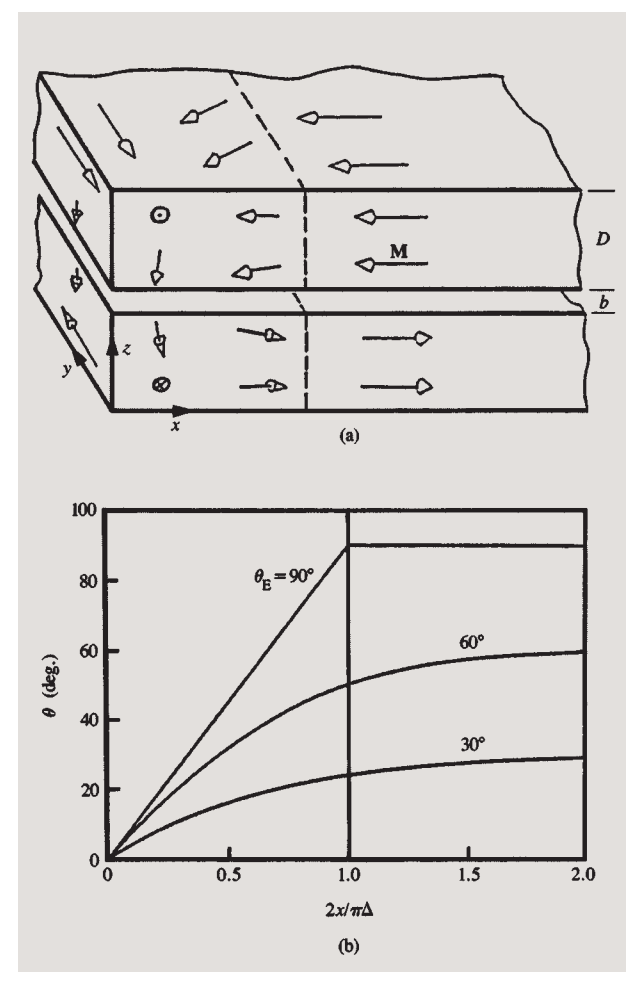
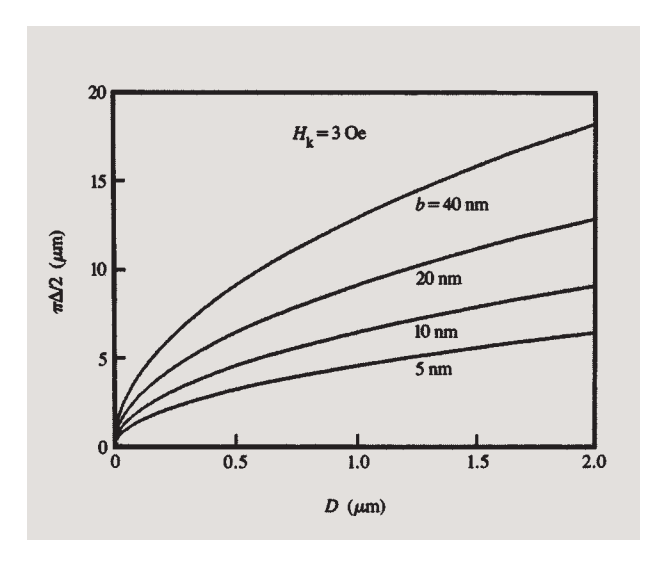


Figure 10

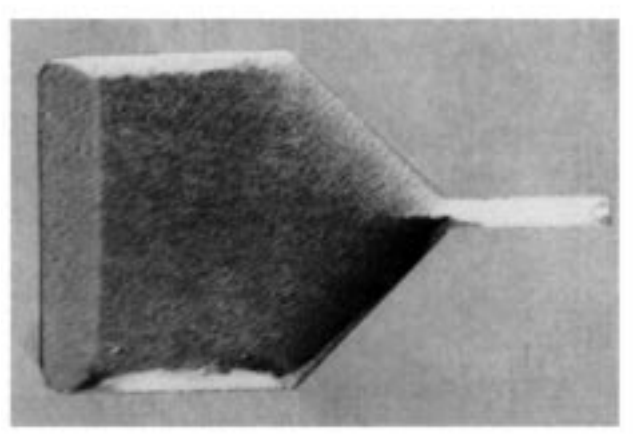
Edge-curling wall (ECW) predictions. (a) Magnetization configuration for $\theta_{\rm E}=90^{\circ}$. (b) In-plane case for three values of $\theta_{\rm E}$. From [12], reproduced with permission. © 1988 IEEE.



Predicted 90° edge-curling wall width $(\pi\Delta/2)$ versus thickness D of magnetic layer and thickness b of spacer layer, for Permalloy, with $H_k=3$ Oe. From [12], reproduced with permission. © 1988 IEEE.

predicts an exponential-like decay of edge curling. This is much more typical of the "tails" predicted for other types of walls from micromagnetic calculations. ECWs have been experimentally verified to exist and have widths of the order of magnitude predicted by the model [12, 47–49, 52, 53]; in an independent study of long laminated stripes, "longitudinally magnetized" (M_L) regions were observed and later identified with ECWs [52]. Typical experimental results are seen in Figure 12, where the ECWs are clearly visible at the upper and lower edges of the yoke.

Should the edge-curling wall width exceed half the width of the laminate, the model predicts that the easy-axis state should be replaced with a new magnetic configuration, in which M is oriented normal to the easy axis. This is the "hard-axis" state of Figure 9(b). M would lie in opposite hard-axis directions on layer pairs. This state, which resembles that of a permanent magnet and has very low permeability, is to be avoided in narrow flux-carrying structures such as pole tips. The pole tips in parts (a) and (b) of Figure 12 are in hard-axis states; the light and dark shading results from the upper magnetic level remaining magnetized alternately to the right and left in different experiments. To avoid the hard-axis state, it is necessary to narrow the ECWs by laminating with multiple thin layers (retaining even numbers of magnetic layers), or by using material with an increased $K^{1/2}/M_s$ ratio. The Bloch wall state of Figure 9(c) occurs if the spacer is too thick, causing the individual layers to flux close in-plane, rather than between layers.



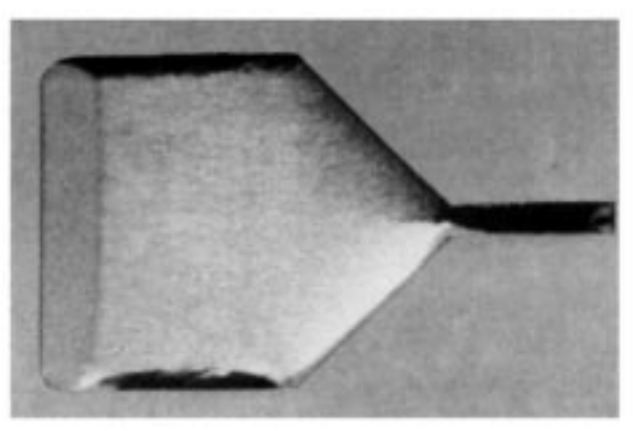


Figure 12

LAMOM images of two-magnetic-layer Permalloy yoke with $D=1~\mu m$ and b=100~Å. The images were obtained by saturating in one hard-axis direction, removing the field, and recording an image; then saturating in the reverse direction and subtracting the resultant image from the first. Contrast reflects change in the horizontal component of magnetization; reversing the field directions gives opposite contrast. Edge-curling walls may be seen at the upper and lower edges. The pole tip was in the "hard-axis" state. By the courtesy of B. Petek.

• Coupled-wall states

All three predicted states are seen experimentally. In the easy-axis case, the edge-curling wall widths observed are in reasonable agreement with the model, and there is good correlation between the observed states in Permalloy elements and the phase diagrams of [12]: Phase diagrams predicting the states for Permalloy elements of a given width ($\theta_{\rm E}=90^{\circ}$) as a function of b and D are presented. However, finite laminated elements, in the easy-axis state, are not usually found to be single-domain. Instead, easy-axis regions separated by 180° walls (without triangular-closure domains) are usually observed. An example is seen in the laminated yoke of Figure 8, where a single 180° (Bloch) wall is observed near the back of the yoke. Such

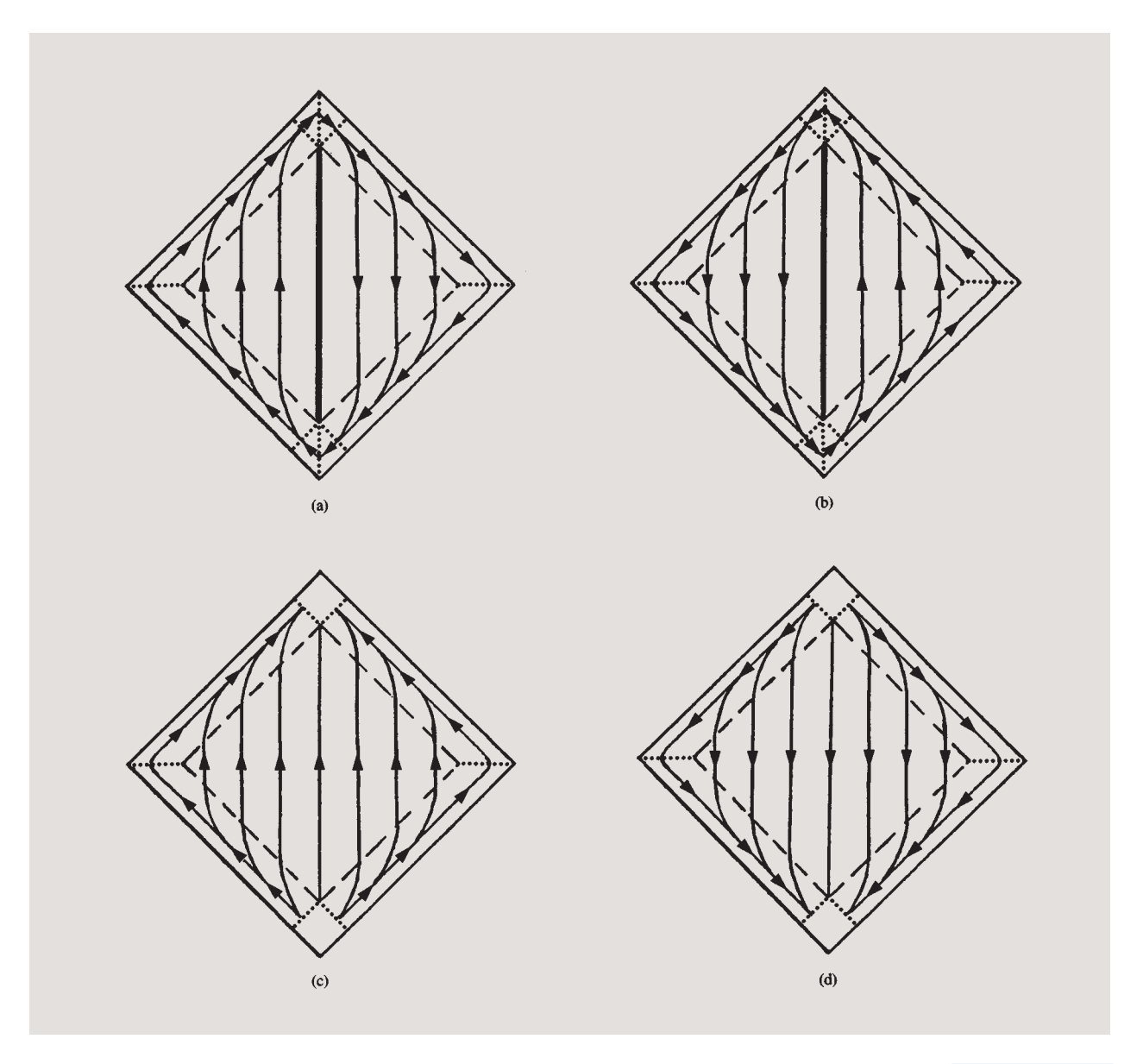


Figure 13

One-wall states (a, b) and single-domain (c, d) states in a laminated diamond-shaped element prepared by plating. Both layers are visualized from above. From [44], reproduced with permission. © 1987 IEEE.

"domained" or "coupled-wall" states, though not included in the model, have been established experimentally [47, 48]. Single-domain, easy-axis states are observed, but, in the small elements studied, they tend not to be the most stable states in the presence of external magnetic fields. Schematic interpretations of M orientation for single-domain and one-wall coupled states in diamond-patterned structures are shown in Figure 13. Note that the senses of circulation in the edge-curling walls of the one-wall state depicted in parts (a) and (b) are continuous. In contrast,

there must be discontinuities in edge-curling at the top and bottom corners of the single-domain state, as shown in parts (c) and (d). These discontinuities have been imaged and are thought to be contributors to the lesser stability of the single-domain state, compared with the one-wall state, in the presence of an external field (see [48]).

A study of long laminated stripes [52] noted jumps (creep) in the magnetoresistive response, which were shown to be related to reversals (discontinuities) in circulation of the edge-curling walls (M_L regions). Such a

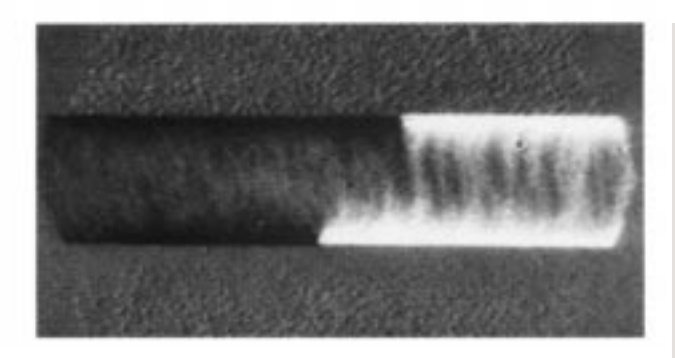


Figure 14
Reversal in ECWs. By the courtesy of C. Tsang and B. Petek.

reversal has been captured in the image shown in Figure 14. The jumps became smaller and the overall hysteresis was reduced with multiple lamination, reflecting the increased number of narrower ECWs (and the increased number of nearly degenerate remanent states). In addition, ECW effects prevented the use of simple transverse biasing to suppress non-single-domain behavior. Other authors have also observed and modeled the nucleation and migration of switching transitions in the ECWs in narrow laminated Permalloy stripes [53].

• Permeance roll-off with frequency

The frequency dependence of the permeance of laminated material was studied both theoretically and experimentally [54]. By using a mean-field technique, a Fourier series solution to the wave equation for laminated geometries was found [54]. Both resistive and capacitive coupling were included in the analysis. The experimental results obtained showed that the permeance roll-off frequency increases with lamination, even with conductive nonmagnetic layers (Figure 15). Roll-off frequency was also found to increase with spacer resistivity. Results were in reasonable agreement with theory, including resonances in permeance due to interference effects related to dimensions (Figure 16).

• Edge-closed lamination (ECL)

Preliminary work is being done on a new form of lamination with flux closure at the edges via soft-magnetic closure layers [55]. This approach avoids the micromagnetic edge-closure wall structure and many of the related problems. A cross section of the structure is seen in Figure 17. Flux closure occurs via edge-closure layers having the same saturation moment (same thickness D, if the same material) as the magnetic layers. In response to promising experimental results [55], a model was

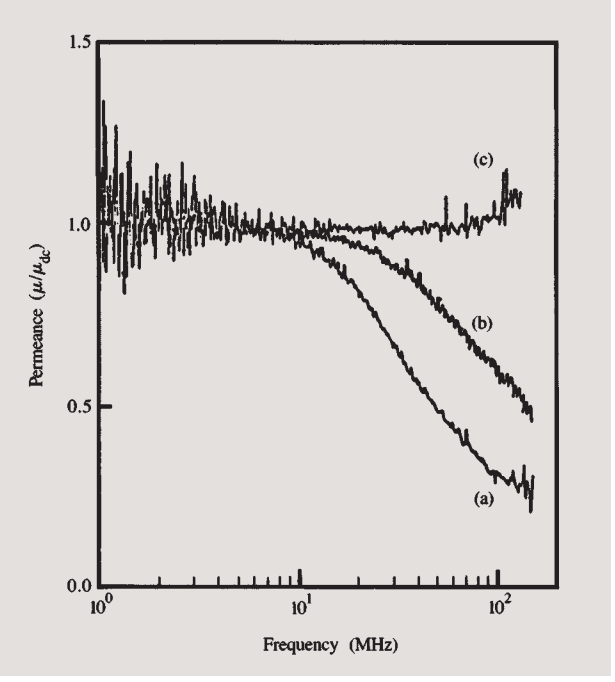


Figure 15

Frequency-dependence of (a) monolithic $\mathrm{Ni_{80}Fe_{20}}$, 1.5 $\mu\mathrm{m}$ thick; (b) laminated $\mathrm{Ni_{80}Fe_{20}}$ consisting of fifteen 1000-Å-thick $\mathrm{Ni_{80}Fe_{20}}$ layers separated by fourteen 100-Å-thick Zr layers; and (c) laminated $\mathrm{Ni_{80}Fe_{20}}$ consisting of fifteen 1000-Å-thick $\mathrm{Ni_{80}Fe_{20}}$ layers separated by fourteen 100-Å-thick $\mathrm{SiO_{2}}$ layers. From [54], reproduced with permission. © 1990 IEEE.

developed for ECL [56], which has been substantially verified. Key results of this work include indications that

- An easy-axis (EA) state, without ECWs, can be achieved with proper choices of materials parameters and dimensions.
- In contrast to simple lamination, increased spacer thickness does not harm the EA state; the narrower the strip being laminated, the greater the preferred spacer thickness.
- The EA state is quite robust in the face of imperfect structure fabrication. As examples, if the spacer layer is somewhat thinner than the minimum for the EA state with no flux leakage through the spacer, or if flux closure is less than 100% through the edge-closure layers, the resultant states evidence, respectively, vestigial ECWs (with a few degrees of edge curling), or vestigial Blochwall states, with small, unconnected edge-closure domains. If such imperfections are not too severe, these states conduct flux nearly as well as the EA state.

Permeance resonances due to interference when film width is equal to odd half-wavelengths, shown (magnitude and phase) for films that were 1.2, 0.5, 0.3, and 0.2 cm wide. The first resonance shifted upward with decreasing film width. For a 1.2-cm-wide film the n=1-, n=3-, and n=5-order resonances were visible. Jagged lines represent data; solid lines represent calculated behavior at $f_0=5$ MHz and $f_c=260$ THz. From [54], reproduced with permission. © 1990 IEEE.

Figure 18 shows a typical domain pattern for an ECL flat yoke and pole tip shape. In this structure, the most stable micromagnetic state in the open yoke area was found to be the single domain shown in part (a). The pole tip region contained a few 180° walls, as shown in parts (a) and (b); on closer inspection, these walls were seen to have small closure domains at the ends, as predicted [56] for incomplete flux closure through the edge layers. After the pole tip was saturated, a state with a different number of walls could sometimes be induced. To study the dynamic stability of the EA state, experimental heads with

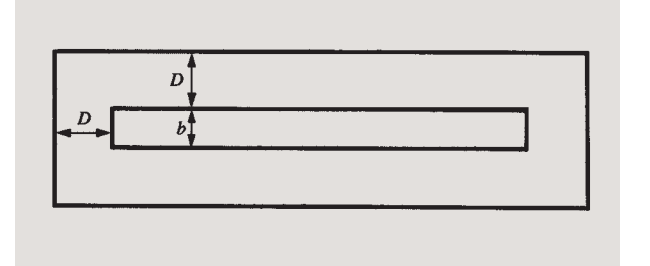


Figure 17

Cross section of edge-closed structure. From [55], reproduced with permission.

ECL top yokes and pole tips were fabricated and the domains in the top yokes were observed under excitation equivalent to "write" conditions. The EA state was found to be stable under drives up to twice the write amplitude.

• Deposition of laminated soft-magnetic materials
Experiments to date have been directed at a number of electroplated and sputtered materials. Work has been reported on electroplated samples including NiFe laminated from separate baths with NiP [12, 47, 48, 55], and NiFe with a small component of Cu laminated with Cu from a single bath by current modulation [46, 57].

A number of studies with laminations that were vacuum-deposited by rf or ion-beam sputtering have been reported. These include NiFe and CoZr laminated with Ta [50, 52], NiFe with SiO₂ and Zr [54], and NiFe with ZrO₂ [54]. A different approach is to sputter reactively with partial substitution of N for Ar as the sputtering gas. With use of this technique, laminations of NiFe with (nonmagnetic) NiFeN [58–60], as well as Fe with FeN [61], which behaves as a laminated soft-magnetic material, have been reported. Other results include NiFe and CoNiFePd laminated with Al₂O₃ [44, 49]. Finally, layers of evaporated NiFe with evaporated Schott glass spacers have also been described [46].

Exchange anisotropy in sputtered NiFe/FeMn films

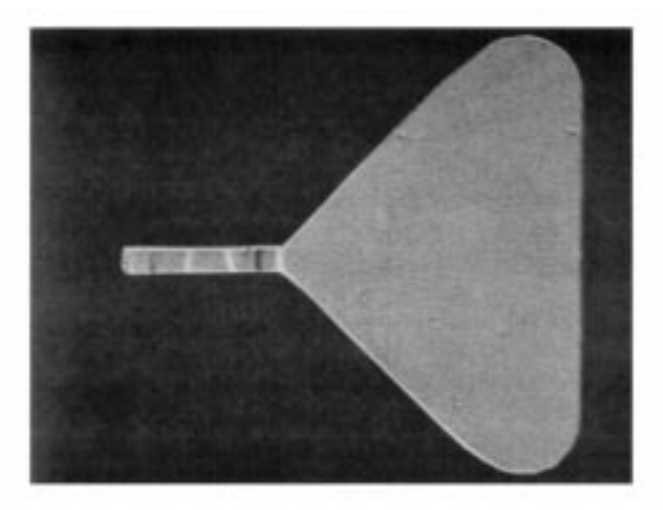
Magnetoresistive (MR) sensors [62–64] enjoy a number of advantages over inductive read heads. Since MR sensors detect magnetic flux directly, their output amplitude is independent of the relative speed between the head and the recording medium. In addition, the output is proportional to the sensing current, typically producing signals higher than obtained with inductive heads. However, a small MR sensor of, e.g., patterned Permalloy is typically broken up into domains to reduce

magnetostatic energy. Under the influence of an external field, the domain walls move in discontinuous Barkhausen jumps, producing irregular and noisy output. The problem can be minimized by rendering the Permalloy into a single-domain state so that it responds to the field by coherent rotation rather than by domain wall motion.

One method of eliminating domains is by coupling the Nig1Fe19 layer to an antiferromagnetic layer such as Fe₅₀Mn₅₀ [63]. The antiferromagnetic (AF) layer is deposited on the ferromagnetic (F) layer in the same pumpdown in order to create an interfacial exchange coupling between the F and AF layers. The spin structure of the AF layer can be aligned along a desired direction (in the plane of the films) by heating beyond the blocking temperature of the AF layer and cooling in the presence of a magnetic field [65, 66]. The blocking temperature $T_{\rm B}$ is the temperature at which the exchange anisotropy vanishes because the local anisotropy of the antiferromagnet, which decreases with temperature, has become too small to anchor the AF spins to the crystallographic lattice. For temperatures below the blocking temperature, the hysteresis loop of the F layer is shifted from the origin by an effective exchange-bias field, H_{ϵ} , with a corresponding unidirectional exchange anisotropy energy constant, $K_{e} = Mt_{E}H_{e}$, where M and t_{E} are the saturation magnetization and thickness of the F layer, respectively. The linear dependence of H_{\star} on inverse NiFe thickness has been verified down to a thickness of 25 Å [67-71]. For NiFe thicknesses below 25 Å, H_a decreases rapidly, reaching zero at a thickness of 8 Å [70], although for this thickness the magnetization decreases by only 30%.

Considerable activity has been devoted to understanding the NiFe/FeMn system, since the size of the observed exchange anisotropy is two orders of magnitude smaller than expected from simple models. In the simplest model [65], the AF spin structure is represented by sheets parallel to the interface and with all spins parallel within each sheet; adjacent sheets are oriented antiparallel to each other. At the interface the sheet of F spins is coupled by exchange to the sheet of AF spins. If the interfacial exchange coupling were comparable to atomic exchange coupling in the bulk F or AF material, its value would be $\approx 10^{-14}$ erg/atom or ≈ 10 erg/cm² of interface area [71, 72]. However, in sputtered NiFe/FeMn couples the observed exchange anisotropy constant K_{α} is only $\approx 0.1 \text{ erg/cm}^2$. A reduction by a factor of 3 to 5 is expected from the noncollinear spin structure [73, 74] of y-phase FeMn and from local variations in grain orientation. A further reduction by at least a factor of 3 is expected because of the inhomogeneity of the FeMn layer, as discussed below.

Sputtered FeMn films have a tendency to change from the metastable γ -phase to the nonmagnetic (at room temperature) α -phase [63]. Thus Fe₅₀Mn₅₀ forms in the α -phase when sputtered on amorphous substrates. The



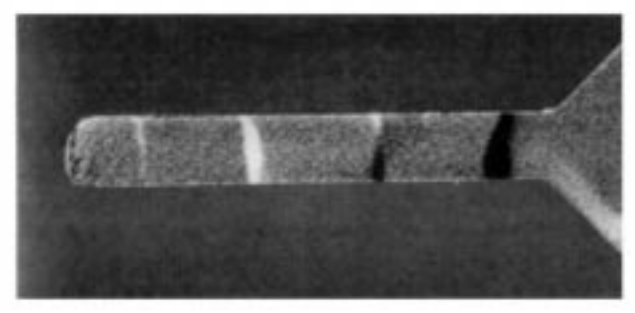


Figure 18

LAMOM images of edge-closed yoke and pole tip. From [55], reproduced with permission.

y-phase can be stabilized [63] by sputtering FeMn onto conforming y-phase underlayers, such as Ni₈₁Fe₁₀ or Cu, whose lattice parameters are close to that of γ-FeMn. Even in these cases the y-phase is maintained only over the initial ~100 Å adjacent to the interface with the underlayer [75]. Reactive sputtering in an Ar-N, plasma has been successfully used to grow the y-phase directly on glass [76] up to thicknesses of 5000 Å. In the same study, a 2500-Å-thick FeMn(N) layer was used as an epitaxial nucleation layer for the deposition of 400 Å Fe₅₀Mn₅₀/400 Å NiFe. By varying the N, partial pressure, the lattice parameter of the FeMn(N) layer was adjusted to the value of bulk 7-Fe₅₀Mn₅₀, resulting in the increase of the exchange anisotropy energy up to 0.22 erg/cm². The authors attributed the increase to an epitaxial relationship between the y-FeMn layer and the y-FeMn(N) nucleation layer. Since the exchange interaction is on the atomic scale, an epitaxial relationship between F and AF layers was believed to be critical. Figure 19 shows a crosssectional TEM image of the NiFe/FeMn interface [75]. Moiré fringes are seen to extend continuously across the



Figure 19

Cross-sectional TEM image of the FeMn/NiFe interface, showing Moiré fringes running continuously across the interface. From [75], reproduced with permission.

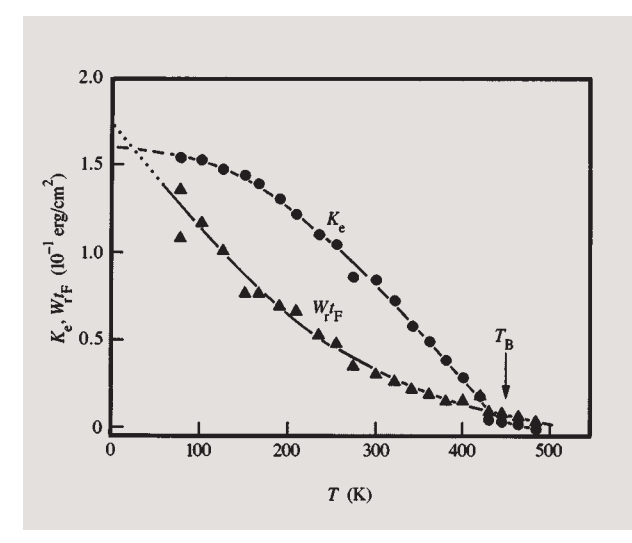


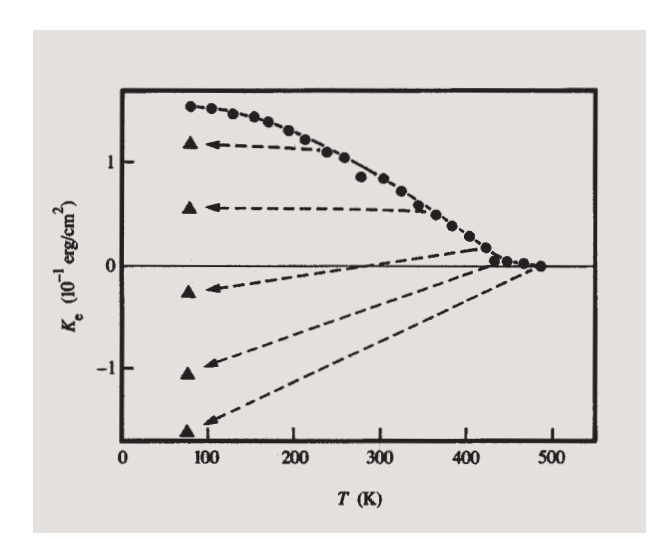
Figure 20

Unidirectional anisotropy $K_{\rm e}$ and rotational hysteresis $W_{\rm r}I_{\rm F}$, measured upon warming for a 400 Å NiFe/200 Å FeMn structure. From [78], reproduced with permission. © 1990 IEEE.

NiFe/FeMn interface. The continuity of the fringes strongly suggests that the grains of γ -FeMn grow epitaxially on the NiFe grains. The lattice misfit of 2.5% between γ -FeMn and NiFe is largely accommodated by coherent elastic strain, without the formation of dislocations. The presence of elastic strain may account for the change from the γ -phase to the α -phase for film thicknesses above $\sim 100 \text{ Å}$ [75].

Torque measurements of sputtered NiFe/FeMn films have demonstrated that the inhomogeneity of the FeMn layer is at least partly responsible for the low magnitude of the exchange anisotropy K_e [77, 78]. Figure 20 shows K_e and rotational hysteresis $W_r t_F$ versus temperature for 400 Å NiFe/200 Å FeMn/200 Å Ta. The sample was annealed for one hour at 515 K before cooling to 77 K in the presence of a 200-Oe field, and was measured upon warming. As can be seen, $K_{\rm a}$ and $W_{\rm r}t_{\rm F}$ were of comparable magnitude, and both increased with decreasing temperature. Nonzero rotational hysteresis implies the presence of FeMn regions which are exchange-coupled to the NiFe but whose local coercivity is too small to keep the spins anchored to the crystallographic lattice. In other words, these regions cannot be blocked even at low temperature. At low temperature, $W_{\rm r}t_{\rm F} \simeq K_{\rm e}$. As a result, for coherent rotation, the volume fraction of unblockable regions is at least equal to the fraction which can be blocked [78], implying at least a factor of 2 reduction in K_{\bullet} from the value it would have if all regions were blocked. Moreover, the switching in the AF layer is likely to occur by incoherent rotation or domain-wall motion, which would significantly decrease the rotational hysteresis per region. Thus, it is likely that the fraction of unblockable volume is larger than 50%, giving a correspondingly larger reduction in K_{α} . Of the regions which are blocked at low temperature, many become free to rotate as the temperature increases. Sputtered NiFe/FeMn films are characterized by a broad distribution in local blocking temperatures [63, 78, 79]. The closed circles in Figure 21 show the variation of K_0 upon warming, as described above. The triangles show K_{ϵ} measured at 77 K after field-cooling to 77 K along the easy direction, warming to higher temperatures, applying a 10-kOe field antiparallel to the easy direction, and then cooling again to 77 K. Negative values of K_a indicate that the easy direction had rotated by 180°. The dashed lines indicate the temperatures at which the reverse field was applied during cooling. Since K_a at 77 K can be decreased by field-cooling from temperatures lower than the peak blocking temperature, it is clear that the sample had a range of local blocking temperatures.

Regions with different local blocking temperatures contribute to the net exchange anisotropy as independent particles [78]. As shown schematically in Figure 22(a), there are separate regions within the FeMn layer, each contributing to the net exchange anisotropy. The NiFe



Unidirectional anisotropy $K_{\rm e}$ versus temperature for 400 Å NiFe/200 Å FeMn structure. Closed circles represent data obtained upon warming; closed triangles represent data obtained at 77 K after cooling in a reverse field from temperatures at right ends of dashed lines. From [78], reproduced with permission. © 1990 IEEE.

layer, because of its strong self-exchange interaction, remains rigid and, as indicated in Figure 22(b), sums the local contributions [78]. The summation is vectorial, since the exchange interaction is of the form $S_F S_{AF}$ cos θ , where S_F and S_{AF} are the spins and θ is the angle between the F and AF spins. If only one local contributor is rotated by 90° by appropriate field cooling, the magnitude of the net anisotropy should decrease, while the easy direction should change by an angle $\Delta \phi_0$. For any field-cooling angle, the relationship between K_e and $\Delta \phi_0$ can easily be calculated and compared with experiment. For example, in Figure 23(a), the cooling angle was 150°, while in Figure 23(b), it was 75°. Good agreement between measured points and calculated curves is clearly evident.

The results discussed above account for about an order of magnitude reduction in $K_{\rm e}$. A different model consistent with the observed low value of $K_{\rm e}$ invokes random exchange fields due to monatomic steps at the F/AF interface [71, 72]. Surface roughness leads to alternating AF spin orientation in contact with the F spins. The net exchange anisotropy is then the result of averaging along the interface, and varies inversely with the size of the averaging area. In this model, the existence of bubble-like domains in the AF layer is postulated, with domain walls perpendicular to the interface. The size of the domains is determined by balancing the domain wall energy against the net exchange anisotropy energy. The main result

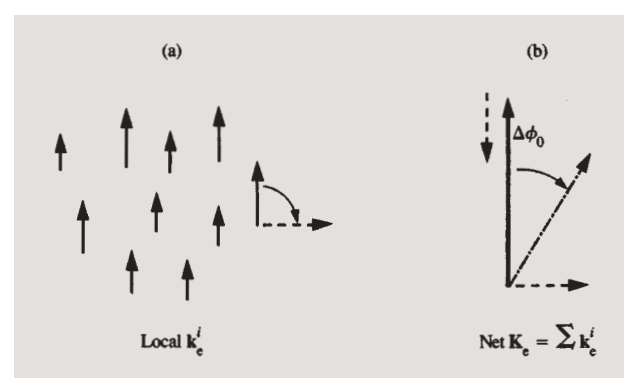


Figure 22

Schematic representation of top view of local exchange anisotropies \mathbf{k}_e^i before and after rotation of a single particle. The net anisotropy \mathbf{K}_e changes in both magnitude and direction.

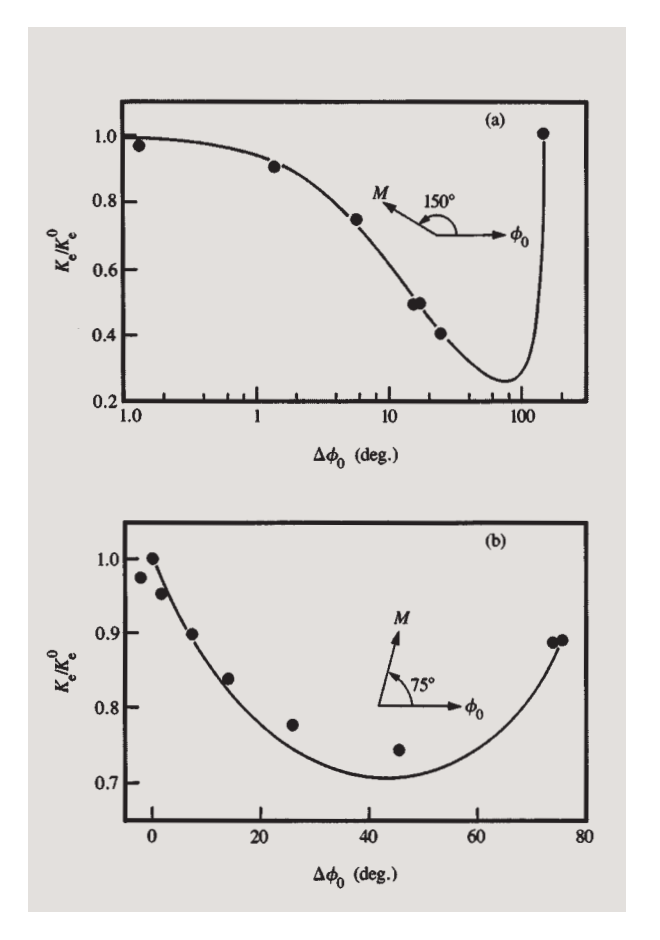


Figure 23

Comparison between measured (solid circles) and calculated lines of exchange anisotropy versus the change in easy direction for field cooling at (a) 150° and (b) 75° to the initial easy direction. From [78], reproduced with permission. © 1990 IEEE.

obtained from this model is that the exchange anisotropy energy should vary as the energy of a domain wall in the AF layer, rather than as the strength of local atom-to-atom exchange coupling along the interface.

Magnetic multilayer structures

Magnetic multilayer structures with periods as low as 20 Å are emerging as a new class of magnetic structures whose properties are different from those of their constituent sublayers taken individually. For example, multilayer structures of ultrathin Fe/Cr films exhibit magnetoresistances with room-temperature amplitudes as high as 15% for films deposited by molecular beam epitaxy [80] and 11% for films deposited by sputtering [81-83]. A new form of exchange coupling maintains the Fe sublayers oriented antiparallel to one another so that saturation fields as high as 20 kOe are observed. The change in resistance is associated with the relative change in the alignment of the magnetizations of the Fe sublayers, and is independent of the angles between the magnetizations and the current. The effect is thus fundamentally different from the usual anisotropic magnetoresistance seen in metallic ferromagnets. The large magnetoresistance in Fe/Cr multilayer structures is of interest because it suggests the potential use of such structures as field sensors.

Concluding remarks

We have reviewed recent advances in magnetic thin films used in recording technology, emphasizing the work done at IBM. As the density of magnetic data storage has increased, magnetic and mechanical scaling requirements regarding thin films used in recording media and heads have become increasingly stringent. Recent years have seen the development of very thin (~200-Å-thick) longitudinal recording media based on Co alloys with magnetic properties necessary to achieve higher densities. The important concept that the media noise level can be reduced by decreasing or eliminating magnetic exchange coupling between grains has been established by a combination of powerful micromagnetic computation, highresolution transmission electron microscopy, and Lorentz and magnetic force microscopy imaging of recorded transitions. In the field of soft-magnetic materials, the challenge has been to maintain high permeability as the dimensions of inductive thin-film recording heads are reduced. Shrinking track widths increases the relative influence of domains, leading to larger nonlinear, irreversible characteristics in head response. By allowing flux closure between layers rather than within each layer, lamination of magnetic and nonmagnetic materials provides one way to simplify the domain structure, thereby giving improved performance. Looking to the future, magnetoresistive sensors using very thin NiFe film elements exchange-coupled to antiferromagentic FeMn

layers show promise for disk storage applications, although the observed magnitude of the exchange coupling has yet to be fully understood. Finally, magnetic multilayer structures with periods as low as 20 Å are emerging as a new class of magnetic structures whose properties may be tailored to fit device requirements.

Acknowledgments

We are grateful to L. P. Franco and J. Mamin of the IBM Almaden Research Center for providing unpublished data; to P. S. Alexopoulos of the IBM Almaden Research Center for Lorentz micrographs; and to B. Petek of the IBM Thomas J. Watson Research Center for LAMOM images. We are indebted to J. K. Howard and C. Hwang of the IBM San Jose facility, to B. Gurney and S. S. P. Parkin of the IBM Almaden Research Center, and to J. C. Slonczewski, L. T. Romankiw, B. E. Argyle, P. L. Trouilloud, and B. Petek of the IBM Thomas J. Watson Research Center for stimulating discussions.

References and notes

- 1. S. Iwasaki, IEEE Trans. Magn. MAG-16, 71 (1980).
- S. Iwasaki and Y. Nakamura, *IEEE Trans. Magn.* MAG-13, 1272 (1977).
- 3. I. A. Beardsley, IEEE Trans. Magn. MAG-18, 1191 (1982).
- Magnetic Recording, C. D. Mee and E. D. Daniel, Eds., McGraw-Hill Book Co., Inc., New York, 1987.
- M. L. Williams and R. L. Comstock, AIP Conf. Proc. 5, 738 (1971).
- B. K. Middleton and C. D. Wright, IERE Conf. Video & Data Recording 54, 181 (1982).
- T. Chen and T. Yamashita, *IEEE Trans. Magn.* 24, 2700 (1988).
- 8. T. Chen, IEEE Trans. Magn. MAG-17, 1181 (1981).
- S. E. Lambert, I. L. Sanders, A. M. Patlach, and M. T. Krounbi, IEEE Trans. Magn. MAG-23, 3690 (1987).
- 10. E. J. Yarmchuk, IEEE Trans. Magn. MAG-22, 877 (1986).
- 11. I. L. Sanders and S. E. Lambert, *IEEE Proc. VLSI & Computer Peripherals* 1-12, 27 (1989).
- J. C. Slonczewski, B. Petek, and B. E. Argyle, *IEEE Trans. Magn.* 24, 2045 (1988).
- J. Kishigami, K. Itoh, and Y. Koshimoto, *IEEE Trans. Magn.* 24, 2841 (1988).
- J. K. Howard, R. Ahlert, and G. Lim, J. Appl. Phys. 61, 3834 (1987).
- 15. J. K. Howard, J. Appl. Phys. 63, 3263 (1988).
- T. Yogi, G. L. Gorman, C. Hwang, M. A. Kakalec, and S. E. Lambert, *IEEE Trans. Magn.* 24, 2727 (1988).
- 17. J. Zhu and H. N. Bertram, J. Appl. Phys. 63, 3248 (1988).
- J. Zhu and H. N. Bertram, *IEEE Trans. Magn.* 24, 2706 (1988).
- B. R. Natarajan and S. E. Murdoch, *IEEE Trans. Magn.* 24, 2724 (1988).
- J. A. Christner, R. Ranjan, R. L. Peterson, and J. I. Lee, J. Appl. Phys. 63, 3260 (1988).
- K. E. Johnson, P. R. Ivett, D. R. Timmons, M. Mirzamaani, S. E. Lambert, and T. Yogi, *J. Appl. Phys.* 76, 4868 (1990).
- I. L. Sanders, T. Yogi, J. K. Howard, S. E. Lambert, G. L. Gorman, and C. Huang, *IEEE Trans. Magn.* 25, 3869 (1989).
- I. L. Sanders, J. K. Howard, S. E. Lambert, and T. Yogi, J. Appl. Phys. 65, 1234 (1989).
- B. R. Natarajan and S. E. Murdoch, *IEEE Trans. Magn.* 24, 2724 (1988).

- M. Chen, M. A. Kakalec, K. Ju, C. Tsang, and G. Castillo, *IEEE Trans. Magn.* 24, 2988 (1988).
- P. S. Alexopoulos and R. H. Geiss, *IEEE Trans. Magn.* MAG-22, 566 (1986).
- D. W. Abraham, C. C. Williams, and H. K. Wickramasinghe, Appl. Phys. Lett. 53, 1446 (1988).
- H. J. Mamin, D. Rugar, J. E. Stern, B. D. Terris, and S. E. Lambert, *Appl. Phys. Lett.* 53, 1563 (1988).
- H. Aoi, R. Tsuchiya, Y. Shiroishi, and H. Matsuyama, IEEE Trans. Magn. 24, 2715 (1988).
- S. Hasegawa, T. Kawasaki, J. Endo, A. Tonomura, Y. Honda, M. Futamoto, F. Kugiya, and M. Koizumi, J. Appl. Phys. 65, 2000 (1989).
- H. C. Tong, R. Ferrier, P. Chang, J. Tzeng, and K. L. Parker, IEEE Trans. Magn. MAG-20, 1831 (1984).
- H. J. Mamin, D. Rugar, S. E. Lambert, L. P. Franco, I. L. Sanders, and T. Yogi, "Magnetic Force Microscopy of Recording Media," presented at the Conference on Magnetism and Magnetic Materials, Boston, MA, 1989.
- D. Rugar, H. J. Mamin, P. Guethner, S. E. Lambert, J. E. Stern, I. McFadyen, and T. Yogi, J. Appl. Phys. 68, 1169 (1990).
- 34. T. Yógi, C. Tsang, G. Castillo, G. L. Gorman, K. Ju, and T. Nguyen, *IEEE Trans. Magn.* 26, 2271 (1990).
- C. Tsang, M. M. Chen, T. Yogi, and K. Ju, *IEEE Trans. Magn.* 26, 1689 (1990).
- T. D. Howell, D. P. McCown, T. A. Diola, Y. S. Tang, K. R. Hense, and R. L. Gee, *IEEE Trans. Magn.* 26, 2298 (1990).
- S. Katayama, T. Tsuno, K. Enjoji, N. Ishii, and K. Sono, IEEE Trans. Magn. 24, 2982 (1988).
- S. E. Lambert, J. K. Howard, and I. L. Sanders, *IEEE Trans. Magn.* 26, 2706 (1990); E. S. Murdock, B. R. Natarajan, and R. G. Walmsley, *IEEE Trans. Magn.* 26, 2700 (1990).
- 39. L. F. Shew, *IEEE Trans. Electron Computers* EC-12, 383 (1963).
- W. Kullmann, E. Koester, and C. Dorsch, *IEEE Trans. Magn.* MAG-20, 420 (1984).
- H. A. M. van den Berg, K. Schuster, G. Rupp, A. Schone-Warnefeld, and W. Marko, *IEEE Trans. Magn.* 25, 3344 (1989).
- N. R. Belk, P. K. George, and G. S. Mowry, J. Appl. Phys. 59, 557 (1986).
- E. M. T. Velu and D. N. Lambeth, presented at the Conference on Magnetism and Magnetic Materials, San Diego, CA, 1990.
- K. Mitsuoka, S. Sudo, N. Narishige, M. Hanazono, Y. Sugita, K. Koike, H. Matsuyama, and K. Hayakawa, IEEE Trans. Magn. MAG-23, 2155 (1987).
- J.-P. Lazzari and I. Melnick, *IEEE Trans. Magn.* MAG-7, 146 (1971); also, D. Augier and J.-P. Lazzari, *IEEE Trans. Magn.* MAG-7, 679 (1971).
- J. S. Y. Feng and D. A. Thompson, *IEEE Trans. Magn.* MAG-13, 1521 (1977).
- D. A. Herman, B. E. Argyle, P. L. Trouilloud, B. Petek, L. T. Romankiw, P. C. Andricacos, S. Krongelb, D. L. Rath, D. F. Canaperi, and M. L. Komsa, J. Appl. Phys. 63, 4036 (1988).
- D. A. Herman, P. L. Trouilloud, B. E. Argyle, B. Petek, and L. T. Romankiw, *IEEE Trans. Magn.* 24, 3066 (1988).
- 49. K. Mitsuoka, S. Sudo, M. Sano, K. Nishioka, S. Narishige, and Y. Sugita, *IEEE Trans. Magn.* 24, 2823 (1988); private communication subsequently indicated that heads were very stable and had no "read-back wiggle."
- J. L. Su, M.-M. Chen, J. Lo, and R. E. Lee, J. Appl. Phys. 63, 4020 (1988).
- J. C. Slonczewski and S. Middlehoek, Appl. Phys. Lett. 6, 139 (1965); J. C. Slonczewski, IBM J. Res. Develop. 10, 377 (1966).
- C. Tsang, P. Kasiraj, and M. Krounbi, J. Appl. Phys. 63, 2938 (1988).

- M. Ruhrig, W. Rave, and A. Hubert, J. Magn. Magn. Mater. 84, 102 (1990).
- M. A. Russak, C. V. Jahnes, M. E. Re, B. C. Webb, and S. M. Mirzamaani, *IEEE Trans. Magn.* 26, 2332 (1990).
- D. A. Herman, B. E. Argyle, H.-P. Lee, P. L. Trouilloud, and B. Petek, presented at the Conference on Magnetism and Magnetic Materials, San Diego, CA, 1990.
- 56. J. C. Slonczewski, IEEE Trans. Magn. 26, 1322 (1990).
- L. T. Romankiw and J. D. Olsen, Ext. Abstr. Electrochem. Soc. 89-2, Abstract No. 300, 430 (1989);
 L. T. Romankiw and J. D. Olsen, Proc. Sympos. Magn. Mater., Process & Devices 90-8, 339, L. T. Romankiw and D. A. Herman, Eds., Electrochemical Society, 10 S. Main St., Pennington, NJ, 1990.
- 58. B. C. Webb, M. E. Re, M. Russak, and C. V. Jahnes, to be published in J. Appl. Phys. 69 (1991).
- M. E. Re, B. C. Webb, and K. K. Shieh, Technical Digest, Magnetic Recording Conference, Institute of Electrical and Electronics Engineers, 1990.
- T. Takamori, K. K. Shih, D. B. Dove, R. W. Nywening, and M. E. Re, J. Appl. Phys. 68, 2192 (1990).
- K. K. Shieh, M. E. Re, and D. B. Dove, Appl. Phys. Lett. 57, 412 (1990).
- 62. R. Hunt, IEEE Trans. Magn. MAG-7, 150 (1971).
- 63. R. D. Hempstead, S. Krongelb, and D. A. Thompson, *IEEE Trans. Magn.* MAG-14, 521 (1978).
- 64. C. Tsang, J. Appl. Phys. 55, 2226 (1984).
- W. H. Meiklejohn and C. P. Bean, Phys. Rev. 102, 1413 (1956); 105, 904 (1957).
- 66. W. H. Meiklejohn, J. Appl. Phys. 33, 1328 (1962).
- V. S. Speriosu, S. S. P. Parkin, and C. H. Wilts, *IEEE Trans. Magn.* MAG-23, 2999 (1987).
- D. Mauri, E. Kay, D. Scholl, and J. K. Howard, J. Appl. Phys. 62, 2929 (1987).
- W. Stoecklein, S. S. P. Parkin, and J. C. Scott, *Phys. Rev. B* 38, 6847 (1988).
- S. S. P. Parkin and V. S. Speriosu, to be published in "Magnetic Properties of Low-Dimensional Systems,"
 L. M. Falicov and J. L. Moran-Lopez, Eds., Springer Proceedings in Physics, Springer-Verlag, Berlin, 1990.
- 71. A. P. Malozemoff, Phys. Rev. B 35, 3679 (1987).
- 72. A. P. Malozemoff, J. Appl. Phys. 63, 3874 (1987).
- J. S. Kouvel and J. S. Kasper, J. Phys. Chem. Solids 24, 529 (1963).
- H. Umebayashi and Y. Ishikawa, J. Phys. Soc. Jpn. 21, 1281 (1966).
- C. Hwang, R. H. Geiss, and J. K. Howard, J. Appl. Phys. 64, 6115 (1988).
- J. K. Howard and T. C. Huang, J. Appl. Phys. 64, 6118 (1988).
- V. S. Speriosu and S. S. P. Parkin, presented at the International Conference on Magnetism, Paris, France, 1988.
- V. S. Speriosu and S. S. P. Parkin, Technical Digest, Magnetic Recording Conference, Institute of Electrical and Electronics Engineers, 1990.
- 79. C. Tsang and K. Lee, J. Appl. Phys. 53, 2605 (1982).
- M. N. Baibich, J. M. Broto, A. Fert, F. Nguyen Van Dau, F. Petroff, P. Eitenne, G. Creuzet, A. Friedrich, and J. Chalazelas, *Phys. Rev. Lett.* 61, 2472 (1988).
- S. S. P. Parkin, S. Fan, N. More, and K. P. Roche, J. Appl. Phys. 67, 5931 (1990).
- B. A. Gurney, D. R. Wilhoit, V. S. Speriosu, and I. L. Sanders, *IEEE Trans. Magn.* 26, 2747 (1990).
- R. F. C. Farrow, C. H. Lee, and S. S. P. Parkin, *IBM J. Res. Develop.* 34, 903 (1990, this issue).

Received March 7, 1990; accepted for publication January 31, 1991

Virgil S. Speriosu IBM Research Division, Almaden Research Center, 650 Harry Road, San Jose, California 95120. Dr. Speriosu is Manager of the Magnetic Thin Films Department in Storage Systems and Technology. He received a B.S. in physics in 1976 from Case Western Reserve University and a Ph.D. in applied physics in 1983 from the California Institute of Technology. During 1983 Dr. Speriosu was a Research Fellow at the California Institute of Technology, studying crystalline properties of compositionally modulated structures. The following year he became a Research Staff Member at the IBM San Jose Research Laboratory. His interests include magnetic and transport properties of magnetic multilayers, exchange coupling across interfaces, coercivity mechanisms, ferromagnetic resonance, and magnetoelasticity.

where he worked on thin-film packaging for Josephsontunneling circuit chips. Since 1984, Dr. Yogi has been a member of the Recording Materials Department at the Almaden Research Center, and has worked on magnetic thin films for recording media. He is a member of the American Physical Society.

Dean A. Herman, Jr., IBM Research Division, Thomas J. Watson Center, P.O. Box 218, Yorktown Heights, New York 10598. Dr. Herman is a Research Staff Member and Storage Program Manager for the Manufacturing Research Department. He received a B.S. in engineering from the U.S. Military Academy at West Point, New York, in 1960, and the M.S. and Ph.D. degrees in electrical engineering from Stanford University in 1967 and 1975, respectively. Dr. Herman taught in the Department of Electrical Engineering at West Point for 15 years and was Professor and Deputy Head of the Department prior to joining IBM in 1986. At West Point he taught courses principally in physical electronics and electromagnetic fields, while doing research in magnetic materials and microwave resonance experimental techniques. Since joining IBM, he has experimentally studied the micromagnetics of single and laminated thin films, and helped to develop LAMOM (laser magneto-optic microscope) imaging techniques. His current assignment includes responsibility for coordination of technology transfer from Manufacturing Research in Yorktown Heights to the Storage Systems Product Division's manufacturing sites.

lan L. Sanders IBM Research Division, Almaden Research Center, 650 Harry Road, San Jose, California 95120. Dr. Sanders received the B.Eng(Tech) degree with First Class Honours from the University of Wales in 1974. In 1977 he was awarded the Ph.D. degree for research into magnetic film devices carried out at the Wolfson Centre for Magnetics Technology, University College, Cardiff. From 1977 to 1979 he was a Postdoctoral Fellow in the Exploratory Magnetics Group at the IBM Thomas J. Watson Research Center, Yorktown Heights, New York. In 1979, Dr. Sanders became a member of the research staff at the IBM Research Laboratory, San Jose, California, responsible for the design of components for ion-implanted magnetic bubble devices. From 1982 until 1989 he managed a number of groups working in the field of high-density magnetic recording. He is currently Manager of the Recording Materials Department at the IBM Almaden Research Center, San Jose, where his interests are materials aspects and characteristics of thin-film recording media and the development of novel soft-magnetic materials for data storage applications. Dr. Sanders holds eight patents (has three pending applications) and has published over 40 papers in the field of magnetic storage. He is a senior member of the IEEE.

Tadashi Yogi IBM Research Division, Almaden Research Center, 650 Harry Road, San Jose, California 95120. Dr. Yogi is a Research Staff Member in the Storage and Systems Technology Department. He received his B.S. degree in physics from the University of Hawaii in 1970, and his M.S. and Ph.D. degrees in applied physics from the California Institute of Technology in 1973 and 1976, respectively. In 1980 he joined IBM at the Thomas J. Watson Research Center,